

CONSERVATIVE BAYESIAN MODEL-BASED VALUE EXPANSION FOR OFFLINE POLICY OPTIMIZATION

Jihwan Jeong^{1,3*}, Xiaoyu Wang^{1*}, Michael Gimelfarb^{1,3}, Hyunwoo Kim², Baher Abdulhai¹ & Scott Sanner^{1,3}

¹University of Toronto, ²LG AI Research, ³Vector Institute
 {jihwan.jeong, cnxiaoyu.wang, mike.gimelfarb}@mail.utoronto.ca,
 hwkim@lgresearch.ai, baher.abdulhai@utoronto.ca,
 ssanner@mie.utoronto.ca

ABSTRACT

Offline reinforcement learning (RL) addresses the problem of learning a performant policy from a fixed batch of data collected by following some behavior policy. Model-based approaches are particularly appealing in the offline setting since they can extract more learning signals from the logged dataset by learning a model of the environment. However, the performance of existing model-based approaches falls short of model-free counterparts, due to the compounding of estimation errors in the learned model. Driven by this observation, we argue that it is critical for a model-based method to understand when to trust the model and when to rely on model-free estimates, and how to act conservatively w.r.t. both. To this end, we derive an elegant and simple methodology called conservative Bayesian model-based value expansion for offline policy optimization (CBOP), that trades off model-free and model-based estimates during the policy evaluation step according to their epistemic uncertainties, and facilitates conservatism by taking a lower bound on the Bayesian posterior value estimate. On the standard D4RL continuous control tasks, we find that our method significantly outperforms previous model-based approaches: e.g., MOPO by 116.4%, MOREL by 23.2% and COMBO by 23.7%. Further, CBOP achieves state-of-the-art performance on 11 out of 18 benchmark datasets while doing on par on the remaining datasets.

1 INTRODUCTION

Fueled by recent advances in supervised and unsupervised learning, there has been a great surge of interest in data-driven approaches to reinforcement learning (RL), known as *offline RL* (Levine et al., 2020). In offline RL, an RL agent must learn a good policy entirely from a logged dataset of past interactions, without access to the real environment. This paradigm of learning is particularly useful in applications where it is prohibited or too costly to conduct online trial-and-error explorations (e.g., due to safety concerns), such as autonomous driving (Yu et al., 2018), robotics (Kalashnikov et al., 2018), and operations research (Boute et al., 2022).

However, because of the absence of online interactions with the environment that give correcting signals to the learner, direct applications of *online* off-policy algorithms have been shown to fail in the *offline* setting (Fujimoto et al., 2019; Kumar et al., 2019; Wu et al., 2019; Kumar et al., 2020). This is mainly ascribed to the distribution shift between the learned policy and the *behavior policy* (data-logging policy) over the course of training. For example, in Q -learning based algorithms, the distribution shift in the policy can incur uncontrolled overestimation bias in the learned value function. Specifically, positive biases in the Q function for out-of-distribution (OOD) actions can be picked up during policy maximization, which leads to further deviation of the learned policy from the behavior policy, resulting in a vicious cycle of value overestimation. Hence, the design of offline RL algorithms revolves around how to counter the adverse impacts of the distribution shift while achieving improvements over the data logging policy.

*Equal contribution

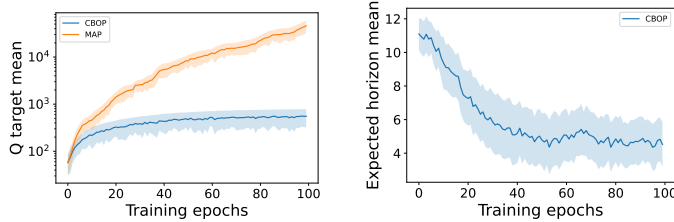


Figure 1: By leveraging the full posterior over the target Q values, CBOP prevents value overestimation. Notably, CBOP can automatically tune the level of reliance on the model-based and bootstrapped Q predictions during training based on their respective uncertainty. (Left) Comparison of the target Q predictions on *hopper-random-v2* dataset from D4RL (Fu et al., 2020). The figure shows that we need the full posterior to counter value overestimation; **MAP** estimation leads to exploding Q values (nb. log scale on the y axis), whereas **CBOP** can safely train the policy. (Right) ‘Expected rollout horizon’ ($\sum_h w_h \cdot h$ with the weight w_h on the h -step TD target computed by model rollouts) of **CBOP** as policy optimization proceeds on *halfcheetah-medium-v2* dataset. Initially, CBOP relies on longer-horizon model-based rollouts; over time as the quality of the Q function improves, the reliance on the model gradually decreases.

In this work, we consider model-based (MB) approaches since they allow better use of a given dataset and can provide better generalization capability (Yu et al., 2020; Kidambi et al., 2021; Yu et al., 2021; Argenson & Dulac-Arnold, 2021). Typically, MB algorithms — e.g., MOPO (Yu et al., 2020), MOREL (Kidambi et al., 2021), and COMBO (Yu et al., 2021) — adopt the Dyna-style policy optimization approach developed in online RL (Janner et al., 2019; Sutton, 1990). That is, they use the learned dynamics model to generate rollouts, which are then combined with the real dataset for policy optimization.

We hypothesize that we can make better use of the learned model by employing it for target value estimation during the policy evaluation step of the actor-critic method. Specifically, we can compute h -step TD targets through dynamics model rollouts and bootstrapped terminal Q function values. In online RL, this MB value expansion (MVE) has been shown to provide a better value estimation of a given state (Feinberg et al., 2018). However, the naïve application of MVE does not work in the offline setting due to model bias that can be exploited during policy learning.

Therefore, it is critical to trust the model only when it can reliably predict the future, which can be captured by the epistemic uncertainty surrounding the model predictions. To this end, we propose CBOP (Conservative Bayesian MVE for Offline Policy Optimization) to control the reliance on the model-based and model-free value estimates according to their respective uncertainties, while mitigating the overestimation errors in the learned values. Specifically, CBOP estimates the Bayesian posterior distribution over a target value from the h -step TD targets for $h = 0, \dots, H$ sampled from the ensemble of the state dynamics and the Q function. Crucially, unlike other approaches such as STEVE (Buckman et al., 2018), CBOP leverages the *full* posterior distribution over target values by estimating a *conservative* lower confidence bound (LCB) on the target value, and thus preventing value overestimation (Figure 1).

We evaluate CBOP on the D4RL benchmark of continuous control tasks (Fu et al., 2020). The experiments show that using the conservative target value estimate significantly outperforms previous model-based approaches: e.g., MOPO by 116.4%, MOREL by 23.2% and COMBO by 23.7%. Further, CBOP achieves state-of-the-art performance on 11 out of 18 benchmark datasets while doing on par on the remaining datasets.

2 BACKGROUND

We study RL in the framework of *Markov decision processes* (MDPs) that are characterized by a tuple $(\mathcal{S}, \mathcal{A}, T, r, d_0, \gamma)$; here, \mathcal{S} is the state space, \mathcal{A} is the action space, $T(s'|s, \mathbf{a})$ is the transition function, $r(s, \mathbf{a})$ is the immediate reward function, d_0 is the initial state distribution, and $\gamma \in [0, 1]$ is the discount factor. Specifically, we call the transition and reward functions the *model* of the environment, which we denote as $f = (T, r)$. A *policy* π is a mapping from \mathcal{S} to \mathcal{A} , and the goal of RL is to find an optimal policy π^* which maximizes the expected cumu-

lative discounted reward, $\mathbb{E}_{\mathbf{s}_t, \mathbf{a}_t} [\sum_{t=0}^{\infty} \gamma^t r(\mathbf{s}_t, \mathbf{a}_t)]$, where $\mathbf{s}_0 \sim d_0, \mathbf{s}_t \sim T(\cdot | \mathbf{s}_{t-1}, \mathbf{a}_{t-1})$, and $\mathbf{a}_t \sim \pi^*(\cdot | \mathbf{s}_t)$. Often, we summarize the quality of a policy π by the state-action value function $Q^\pi(\mathbf{s}, \mathbf{a}) := \mathbb{E}_{\mathbf{s}_t, \mathbf{a}_t} [\sum_{t=0}^{\infty} \gamma^t r(\mathbf{s}_t, \mathbf{a}_t) | \mathbf{s}_0 = \mathbf{s}, \mathbf{a}_0 = \mathbf{a}]$, where actions are sampled according to $\pi(\cdot | \mathbf{s})$.

Off-policy actor-critic methods, such as SAC (Haarnoja et al., 2018) and TD3 (Fujimoto et al., 2018), have enjoyed great successes in complex continuous control tasks in deep RL, where parameterized neural networks for the policy π_θ (known as actor) and the action value function Q_ϕ (known as critic) are maintained. Following the framework of the *generalized policy iteration* (GPI) (Sutton & Barto, 2018), we understand the actor-critic algorithm as iterating between (i) policy evaluation and (ii) policy improvement. Here, policy evaluation typically refers to the calculation of $Q_\phi(\mathbf{s}, \pi_\theta(\mathbf{s}))$ for the policy π_θ , while the improvement step is often as simple as maximizing the currently evaluated Q_ϕ ; i.e., $\max_\theta \mathbb{E}_{\mathbf{s} \sim \mathcal{D}} [Q_\phi(\mathbf{s}, \pi_\theta(\mathbf{s}))]$ (Fujimoto et al., 2018).

Policy Evaluation At each iteration of policy learning, we evaluate the current policy π_θ by minimizing the *mean squared Bellman error* (MSBE) with the dataset \mathcal{D} of previous state transitions:

$$\mathcal{L}(\phi, \mathcal{D}) = \text{MSBE} := \mathbb{E}_{(\mathbf{s}, \mathbf{a}, r, \mathbf{s}') \sim \mathcal{D}} \left[(y(\mathbf{s}, \mathbf{a}, \mathbf{s}') - Q_\phi(\mathbf{s}, \mathbf{a}))^2 \right], \quad (1)$$

$$y(\mathbf{s}, \mathbf{a}, \mathbf{s}') = r(\mathbf{s}, \mathbf{a}) + \gamma Q_{\phi'}(\mathbf{s}', \mathbf{a}'), \quad \mathbf{a}' \sim \pi_\theta(\cdot | \mathbf{s}') \quad (2)$$

where $y(\mathbf{s}, \mathbf{a}, \mathbf{s}')$ is the *TD target* at each (\mathbf{s}, \mathbf{a}) , towards which Q_ϕ is regressed. A separate *target* network $Q_{\phi'}$ is used in computing y to stabilize learning (Mnih et al., 2015). Off-policy algorithms typically use some variations of (2), e.g., by introducing the clipped double- Q trick (Fujimoto et al., 2018), in which $\min_{j=1,2} Q_{\phi'_j}(\mathbf{s}', \mathbf{a}')$ is used instead of $Q_{\phi'}(\mathbf{s}', \mathbf{a}')$ to prevent value overestimation.

Model-based Offline RL In the offline setting, we are given a fixed set of transitions, \mathcal{D} , collected by some *behavior* policy π_β , and the aim is to learn a policy π that is better than π_β . In particular, offline *model-based* (MB) approaches learn the model $\hat{f} = (\hat{T}, \hat{r})$ of the environment using \mathcal{D} to facilitate the learning of a good policy. Typically, \hat{f} is trained to maximize the log-likelihood of its predictions. Though MB algorithms are often considered capable of better generalization than their *model-free* (MF) counterparts by leveraging the learned model, it is risky to trust the model for OOD samples. Hence, MOPO (Yu et al., 2020) and MOREL (Kidambi et al., 2021) construct and learn from a pessimistic MDP where the model uncertainty in the next state prediction is penalized in the reward. Criticizing the difficulty of accurately computing well-calibrated model uncertainty, COMBO (Yu et al., 2021) extends CQL (Kumar et al., 2020) to the model-based regime by regularizing the value function on OOD samples generated via model rollouts. These methods follow the Dyna-style policy learning where model rollouts are used to augment the offline dataset (Sutton, 1990; Janner et al., 2019).

Model-based Value Expansion (MVE) for Policy Optimization Recall the definition of the TD target $y(\mathbf{s}, \mathbf{a}, \mathbf{s}')$ in (2) where we bootstrap from the target value function $Q_{\phi'}(\mathbf{s}', \mathbf{a}')$ which is only an approximation of the true action value $Q^{\pi_\theta}(\mathbf{s}', \mathbf{a}')$. Thus, when the learned model can be trusted, it can help better estimate the target value of the current policy, leading to more efficient policy iteration. Specifically, we can use the h -step MVE target $\hat{R}_h(\mathbf{s}, \mathbf{a}, \mathbf{s}')$ for $y(\mathbf{s}, \mathbf{a}, \mathbf{s}')$:

$$\hat{y}(\mathbf{s}, \mathbf{a}, \mathbf{s}') = \hat{R}_h(\mathbf{s}, \mathbf{a}, \mathbf{s}') := \sum_{t=0}^h \gamma^t \hat{r}_t(\hat{\mathbf{s}}_t, \hat{\mathbf{a}}_t) + \gamma^{h+1} Q_{\phi'}(\hat{\mathbf{s}}_{h+1}, \hat{\mathbf{a}}_{h+1}), \quad (3)$$

$$(\hat{\mathbf{s}}_0, \hat{\mathbf{a}}_0, \hat{r}_0, \hat{\mathbf{s}}_1) = (\mathbf{s}, \mathbf{a}, r, \mathbf{s}'), \quad \hat{\mathbf{s}}_t \sim \hat{T}(\cdot | \hat{\mathbf{s}}_{t-1}, \hat{\mathbf{a}}_{t-1}), \quad \hat{\mathbf{a}}_t \sim \pi_\theta(\cdot | \hat{\mathbf{s}}_t), \quad 1 \leq t \leq h+1,$$

where $\hat{R}_h(\mathbf{s}, \mathbf{a}, \mathbf{s}')$ is obtained by the h -step MB return plus the terminal value at $h+1$ ($h=0$ reduces back to MF). The quality of $\hat{y} = \hat{R}_h(\mathbf{s}, \mathbf{a}, \mathbf{s}')$ as a TD target depends on the qualities of \hat{f} and $Q_{\phi'}$ over the rollout horizon. Naturally, the model becomes less reliable for large h , which has led to the use of small h (Feinberg et al., 2018). In the offline setting, biases in the model can be exploited during policy improvement such that the Q function blows up over the course of training as in Figure 1.

3 CONSERVATIVE BAYESIAN MVE FOR OFFLINE POLICY OPTIMIZATION

The major limitations of MVE when applied to offline RL are two-fold. Firstly, the model predictions $\hat{\mathbf{s}}_t$ and \hat{r}_t become increasingly less credible as t increases because model bias can compound, which results in largely biased target values. Worse yet, we cannot obtain additional on-policy experiences to reduce the model error in the offline setting. Thus, the most common sidestep is to use short-horizon rollouts and rely more on the bootstrapped $Q_{\phi'}$. However, rolling out the model for only a short horizon even when it can be trusted could severely restrict the benefit of being model-based. Secondly, when the model rollouts go outside the support of \mathcal{D} , \hat{R}_h in (3) can have a large overestimation bias, which will eventually be propagated into the learned Q_ϕ function.

Therefore ideally, we would like to **control the reliance on the learned model and the bootstrapped $Q_{\phi'}$ according to their respective epistemic uncertainty, while also preventing Q_ϕ from accumulating large overestimation errors**. In other words, when we can trust \hat{f} more than $Q_{\phi'}$, we can safely roll out the model for more steps to get a better target value estimation. On the contrary, if the model is uncertain about the future it predicts, it is better to shorten the rollout horizon and bootstrap from the $Q_{\phi'}$ function early on. Indeed, Figure 1 (right) exemplifies that CBOP relied much more on the model-based rollouts at the beginning of policy learning because the value function had been just initialized. Gradually as the $Q_{\phi'}$ function becomes more accurate over the course of training, CBOP automatically reduces the weights assigned to longer model-based rollouts.

Below, we present CBOP, a Bayesian take on achieving the aforementioned two goals: trading off the MF and MB value estimates based on their uncertainty while obtaining a conservative estimation of the target $\hat{y}(\mathbf{s}, \mathbf{a}, \mathbf{s}')$. To this end, we first denote the value of the policy π at $(\mathbf{s}_t, \mathbf{a}_t)$ in the learned MDP defined by its dynamics \hat{f} as $\hat{Q}^\pi(\mathbf{s}_t, \mathbf{a}_t)$, or

$$\hat{Q}^\pi(\mathbf{s}_t, \mathbf{a}_t) = \mathbb{E}_{\hat{f}, \pi} \left[\sum_{k=0}^{\infty} \gamma^k \hat{r}(\hat{\mathbf{s}}_{t+k}, \hat{\mathbf{a}}_{t+k}) \right], \quad (\hat{\mathbf{s}}_t, \hat{\mathbf{a}}_t) = (\mathbf{s}_t, \mathbf{a}_t), \quad \hat{\mathbf{a}}_{t+k} \sim \pi(\cdot | \hat{\mathbf{s}}_{t+k}). \quad (4)$$

Then, we view each $\hat{R}_h(\mathbf{s}_t, \mathbf{a}_t, \mathbf{s}_{t+1}) = \sum_{t=0}^h \gamma^t \hat{r}_t(\hat{\mathbf{s}}_t, \hat{\mathbf{a}}_t) + \gamma^{h+1} Q_{\phi'}(\hat{\mathbf{s}}_{h+1}, \hat{\mathbf{a}}_{h+1})$ defined in (3) as a conditionally independent noisy observation of $\hat{Q}^\pi(\mathbf{s}_t, \mathbf{a}_t)$. From this assumption, we can construct the Bayesian posterior over $\hat{Q}^\pi(\mathbf{s}_t, \mathbf{a}_t)$ given the observations $\hat{R}_h(\mathbf{s}_t, \mathbf{a}_t, \mathbf{s}_{t+1}) \forall h$. With the closed-form posterior distribution at hand, we can take various conservative estimates from the distribution; we use the lower confidence bound (LCB) in this work, which we further describe in the next part.

3.1 CONSERVATIVE VALUE ESTIMATION VIA BAYESIAN INFERENCE

Although there exists a unique $\hat{Q}^\pi(\mathbf{s}, \mathbf{a})$ at each (\mathbf{s}, \mathbf{a}) given a fixed model \hat{f} , we cannot directly observe it unless we infinitely roll out the model from (\mathbf{s}, \mathbf{a}) until termination, which is a computationally infeasible option. Instead, we view $\hat{R}_h \forall h$ as (biased) noisy observations of the true underlying parameter \hat{Q}^π .¹ Then, the question becomes how to combine these observations in order to form a better estimator of \hat{Q}^π ? To answer that, we seek the Bayesian posterior estimation of \hat{Q}^π :

$$\mathbb{P}(\hat{Q}^\pi | \hat{R}_0, \dots, \hat{R}_H) \propto \mathbb{P}(\hat{R}_0, \dots, \hat{R}_H | \hat{Q}^\pi) \mathbb{P}(\hat{Q}^\pi) \quad (5)$$

$$= \mathbb{P}(\hat{Q}^\pi) \prod_{h=0}^H \mathbb{P}(\hat{R}_h | \hat{Q}^\pi), \quad (6)$$

where we assume that \hat{R}_h ($h = 0, \dots, H$) are conditionally independent given \hat{Q}^π (see Appendix A where we discuss in detail about the assumptions present in CBOP).

The likelihood of observations $\mathbb{P}(\hat{R}_h | \hat{Q}^\pi)$ and the prior $\mathbb{P}(\hat{Q}^\pi)$ over \hat{Q}^π can be modeled in multiple ways. In this work, we model the likelihood as normally distributed with mean μ_h and variance σ_h^2 ,

$$\hat{R}_h | \hat{Q}^\pi \sim \mathcal{N}(\mu_h, \sigma_h^2). \quad (7)$$

¹We will omit $(\mathbf{s}, \mathbf{a}, \mathbf{s}')$ henceforth if it is clear from the context.

since it leads to a closed-form posterior update. Furthermore, since \hat{R}_h can be seen as a sum of future immediate rewards, when the MDP is ergodic and γ is close to 1, the Gaussian assumption (approximately) holds according to the central limit theorem (Dearden et al., 1998). Also, please note that our Bayesian framework is not restricted to the Gaussian assumptions, and other surrogate probability distributions such as the Student-t distribution could be used instead.

For the prior, we use the improper (or uninformative) prior, $\mathbb{P}(\hat{Q}^\pi) = 1$, since it is natural to assume that we lack generally applicable prior information over the target value across different environments and tasks (Christensen et al., 2011). The use of the improper prior is well justified in the Bayesian literature (Wasserman, 2010; Berger, 1985), and the particular prior we use in CBOP corresponds to the Jeffreys prior, which has the invariant property under a change of coordinates. The Gaussian likelihood and the improper prior lead to a ‘proper’ Gaussian posterior density that integrates to 1, from which we can make various probabilistic inferences (Wasserman, 2010).

The posterior (5) is then normally distributed with mean μ and variance σ^2 as follows:

$$\rho = \sum_{h=0}^H \rho_h, \quad \mu = \sum_{h=0}^H \left(\frac{\rho_h}{\sum_{h=0}^H \rho_h} \right) \mu_h \quad (8)$$

where $\rho = 1/\sigma^2$ and $\rho_h = 1/\sigma_h^2$ are the precisions of the posterior and the Gaussian likelihood over the h -step return, respectively. The posterior mean μ corresponds to the maximum a posteriori (MAP) estimation of \hat{Q}^π . Note that μ has the form of a weighted sum, $\sum_h w_h \mu_h$, with $w_h = \rho_h / \sum_{h=0}^H \rho_h \in (0, 1)$ being the weight allocated to \hat{R}_h .

If the variance of \hat{R}_h for some h is relatively large, we give a smaller weight to that observation. If, on the other hand, \hat{R}_h all have the same variance (e.g. $\rho_0 = \rho_1 = \dots = \rho_H$), we recover the usual H -step return estimate. Recall that the quality of \hat{R}_h is determined by that of the model rollout return and the bootstrapped terminal value. Thus intuitively speaking, the adaptive weight w_h given by the Bayesian posterior allows the trade-off between the epistemic uncertainty of the model with that of the Q function.

Figure 2 illustrates the overall posterior estimation procedure. Given a transition tuple (s, \mathbf{a}, r, s') , we start the model rollout from $s_1 = s'$. At each rollout horizon h , the cumulative discounted reward $\sum_{t=0}^h \gamma^t \hat{r}_t$ is sampled by the dynamics model and the terminal value \hat{Q}_h is sampled by the Q function (the sampling procedure is described in Section 3.2). We then get \hat{R}_h by adding the h -step MB return samples and the terminal values $\gamma^{h+1} \hat{Q}_{h+1}$, which we deem as sampled from the distribution $\mathbb{P}(\hat{R}_h | \hat{Q}^\pi)$ parameterized by μ_h, σ_h^2 (we use the sample mean and variance). These individual h -step observations are then combined through the Bayesian inference to give us the posterior distribution over \hat{Q}^π .

It is worth noting that the MAP estimator can also be derived from the perspective of variance optimization (Buckman et al., 2018) over the target values. However, we have provided much evidence in Section 4 and Appendix D.2 that the point estimate does not work in the offline setting due to value overestimation. Hence, it is imperative that we should have the full posterior distribution over the target value, such that we can make not the MAP estimation but a conservative estimation, which is what CBOP provides.

To further understand the impact of using the MAP estimator for the value estimation, consider an estimator \tilde{Q} of \hat{Q}^π and its squared loss: $L(\hat{Q}^\pi, \tilde{Q}) = (\hat{Q}^\pi - \tilde{Q})^2$. It is known that the posterior mean of \hat{Q}^π minimizes the *Bayes risk* w.r.t. $L(\hat{Q}^\pi, \tilde{Q})$ (Wasserman, 2010), meaning that the posterior risk $\int L(\hat{Q}^\pi, \tilde{Q}) \mathbb{P}(\hat{Q}^\pi | \hat{R}_0, \dots, \hat{R}_H) d\hat{Q}^\pi$ is minimized at $\tilde{Q} = \mu$. In this context, μ is also called the (generalized) *Bayes estimator* of \hat{Q}^π , which is an admissible estimator (Robert, 2007). Despite seemingly advantageous, this result has a negative implication in offline RL. That is, the MAP estimator minimizes the squared loss from $\hat{Q}^\pi(s, \mathbf{a})$ over the entire support of the posterior,

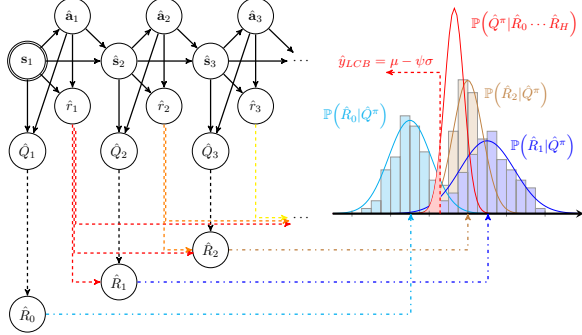


Figure 2: The graphical model representation of CBOP

weighted by the posterior distribution. Now, the distribution shift of π from π_β can lead to significantly biased \hat{Q}^π compared to the true Q^π . In this case, the quality of the MAP estimator when evaluated in the real MDP would be poor. Especially, the overestimation bias in the MAP estimation can quickly propagate to the Q_ϕ function and thereby exacerbate the distribution shift.

3.2 ENSEMBLES OF DYNAMICS AND Q FUNCTIONS FOR SAMPLING H-STEP MVE TARGETS

In this section, we discuss how we estimate the parameters μ_h, σ_h^2 of $\mathbb{P}(\hat{R}_h|\hat{Q}^\pi)$ from the ensemble of dynamics models and that of Q functions.

Assume we have a bootstrapped dynamics ensemble model \hat{f} consisting of K different models ($\hat{f}_1, \dots, \hat{f}_K$) trained with different sequences of mini-batches of \mathcal{D} (Chua et al., 2018; Janner et al., 2019). Similarly, we assume a Q ensemble of size M . Given a state $\hat{\mathbf{s}}_t$ and an action $\hat{\mathbf{a}}_t$, we can construct the probability over the next state $\hat{\mathbf{s}}_{t+1}$ and reward \hat{r}_t by the ensemble as follows:

$$\mathbb{P}(\hat{\mathbf{s}}_{t+1}, \hat{r}_t | \hat{\mathbf{s}}_t, \mathbf{a}_t) = \sum_{k=1}^K \mathbb{P}(\hat{f}_k) \cdot \mathbb{P}(\hat{\mathbf{s}}_{t+1}, \hat{r}_t | \hat{\mathbf{s}}_t, \mathbf{a}_t, \hat{f}_k)$$

where $\mathbb{P}(\hat{f}_k)$ is the probability of selecting the k th model from the ensemble, which is $1/K$ when all models are weighted equally. Now, the sampling method that exactly follows the probabilistic graphical model shown in Figure 2 would first sample a model from the ensemble at each time step, followed by sampling the next state transition (and reward) from the model, which should then be repeated K times per state to generate a single sample. Then, we evaluate the resulting state $\hat{\mathbf{s}}_{t+1}$ and action $\hat{\mathbf{a}}_{t+1} \sim \pi_\theta(\hat{\mathbf{s}}_{t+1})$ with the Q ensemble to obtain M samples. If we want to obtain N trajectories from a single initial state to estimate μ_h and σ_h^2 for $h = 1, \dots, H$, the overall procedure requires $\mathcal{O}(NKH)$ computation, which can quickly become infeasible for moderately large K and N values.

To reduce the computational complexity, we follow Chua et al. (2018) where each *particle* is propagated by a single model of the ensemble for H steps. With this, we can obtain N trajectories of length H from one state with $\mathcal{O}(NH)$ instead of $\mathcal{O}(NKH)$ (below we use $N = K$, i.e., we generate one particle per model). Concretely, given a single transition $\tau = (\mathbf{s}_0, \mathbf{a}_0, r_0, \mathbf{s}_1)$, we create K numbers of *particles* by replicating \mathbf{s}_1 K times, denoted as $\hat{\mathbf{s}}_1^{(k)} \forall k$. The k th particle is propagated by a fixed model \hat{f}_k and the policy π_θ for H steps, where $(\hat{\mathbf{s}}_t^{(k)}, \hat{r}_t^{(k)}) = \hat{f}_k(\hat{\mathbf{s}}_{t-1}^{(k)}, \hat{\mathbf{a}}_{t-1}^{(k)})$ and $\hat{\mathbf{a}}_t^{(k)} \sim \pi_\theta(\hat{\mathbf{s}}_t^{(k)})$. At each imagined timestep $t \in [0, H + 1]$, M number of terminal values are sampled by the $Q_{\phi'}$ ensemble at $(\hat{\mathbf{s}}_t^{(k)}, \hat{\mathbf{a}}_t^{(k)})$.

Despite the computational benefit, an implication of this sampling method is that it no longer directly follows the graphical model representation in Figure 2. However, we can still correctly estimate μ_h and σ_h^2 by turning to the law of total expectation and the law of total variance. That is,

$$\mu_h = \mathbb{E}_{\pi_\theta} [\hat{R}_h | \tau] = \mathbb{E}_{\hat{f}_k} [\mathbb{E}_{\pi_\theta} [\hat{R}_h | \tau, \hat{f}_k]] \quad (9)$$

where the outer expectation is w.r.t. the dynamics ensemble sampling probability $\mathbb{P}(\hat{f}_k) = 1/K$. Hence, given a fixed dynamics model \hat{f}_k , we sample \hat{R}_h by following π_θ and compute the average of the h -step return, which is then averaged across different ensemble models. In fact, the resulting μ_h is the mean of all aggregated $M \times K$ samples of \hat{R}_h .

The MVE target variance $\text{Var}_{\pi_\theta}(\hat{R}_h|\tau)$ decomposes via the law of total variance as following:

$$\sigma_h^2 = \text{Var}_{\pi_\theta} [\hat{R}_h | \tau] = \underbrace{\mathbb{E}_{\hat{f}_k} [\text{Var}_{\pi_\theta} [\hat{R}_h | \tau, \hat{f}_k]]}_A + \underbrace{\text{Var}_{\hat{f}_k} [\mathbb{E}_{\pi_\theta} [\hat{R}_h | \tau, \hat{f}_k]]}_B. \quad (10)$$

Here, A is related to the epistemic uncertainty of the $Q_{\phi'}$ ensemble; while B is associated with the epistemic uncertainty of the dynamics ensemble. The total variance $\text{Var}_{\pi_\theta}(\hat{R}_h|\tau)$ captures both uncertainties. This way, even though we use a different sampling scheme than presented in the graphical model of Figure 2, we can compute the unbiased estimators of the Gaussian parameters.

Table 1: Normalized scores on D4RL MuJoCo Gym environments. Experiments ran with 5 seeds.

		MOPO	MOReL	COMBO	CQL	TD3+BC	EDAC	IQL	CBOP
random	halfcheetah	35.4 ± 2.5	25.6	38.8	35.4	10.2 ± 1.3	28.4 ± 1.0	-	32.8 ± 0.4
	hopper	11.7 ± 0.4	53.6	17.9	10.8	11.0 ± 0.1	31.3 ± 0.0	-	31.4 ± 0.0
	walker2d	13.6 ± 2.6	37.3	7.0	7.0	1.4 ± 1.6	21.7 ± 0.0	-	17.8 ± 0.4
medium	halfcheetah	42.3 ± 1.6	42.1	54.2	44.4	42.8 ± 0.3	67.5 ± 1.2	47.4	74.3 ± 0.2
	hopper	28.0 ± 12.4	95.4	94.9	79.2	99.5 ± 1.0	101.6 ± 0.6	66.2	102.6 ± 0.1
	walker2d	17.8 ± 19.3	77.8	75.5	58.0	79.7 ± 1.8	92.5 ± 0.8	78.3	95.5 ± 0.4
medium replay	halfcheetah	53.1 ± 2.0	40.2	55.1	46.2	43.3 ± 0.5	63.9 ± 0.8	44.2	66.4 ± 0.3
	hopper	67.5 ± 24.7	93.6	73.1	48.6	31.4 ± 3.0	101.8 ± 0.5	94.7	104.3 ± 0.4
	walker2d	39.0 ± 9.6	49.8	56.0	26.7	25.2 ± 5.1	87.1 ± 2.3	73.8	92.7 ± 0.9
medium expert	halfcheetah	63.3 ± 38.0	53.3	90.0	62.4	97.9 ± 4.4	107.1 ± 2.0	86.7	105.4 ± 1.6
	hopper	23.7 ± 6.0	108.7	111.1	98.7	112.2 ± 0.2	110.7 ± 0.1	91.5	111.6 ± 0.2
	walker2d	44.6 ± 12.9	95.6	96.1	111.0	101.1 ± 9.3	114.7 ± 0.9	109.6	117.2 ± 0.5
expert	halfcheetah	-	-	-	-	105.7 ± 1.9	106.8 ± 3.4	-	100.4 ± 0.9
	hopper	-	-	-	-	112.2 ± 0.2	110.3 ± 0.3	-	111.4 ± 0.2
	walker2d	-	-	-	-	105.7 ± 2.7	115.1 ± 1.9	-	122.7 ± 0.8
full replay	halfcheetah	-	-	-	-	-	84.6 ± 0.9	-	85.5 ± 0.3
	hopper	-	-	-	-	-	105.4 ± 0.7	-	108.1 ± 0.3
	walker2d	-	-	-	-	-	99.8 ± 0.7	-	107.8 ± 0.2

Once we obtain μ_h and σ_h^2 , we plug them into (8) to compute the posterior mean and the variance. A conservative value estimation can be made by $\hat{y}_{LCB} = \mu - \psi\sigma$ with some coefficient $\psi > 0$ (Jin et al., 2021; Rashidinejad et al., 2021). Under the Gaussian assumption, this corresponds to the worst-case return estimate in a Bayesian credible interval for Q^π . We summarize CBOP in Algorithm 1 in Appendix B.1.

4 EXPERIMENTS

We have designed the experiments to answer the following research questions: **(RQ1)** Is CBOP indeed able to adaptively determine the weights assigned to different h -step returns according to the relative uncertainty of the learned model and that of the Q function? **(RQ2)** How does CBOP perform in the standard offline RL benchmark compared to previous methods? **(RQ3)** Does CBOP with LCB provide conservative target Q estimation in the offline RL setting? **(RQ4)** How important is it to have the full posterior over the target values versus using the MAP estimation in terms of the final performance? **(RQ5)** How much better is it to adaptively control the weights to h -step returns during training as opposed to using a fixed set of weights throughout training?

We evaluate these RQs on the standard *D4RL* offline RL benchmark (Fu et al., 2020). In particular, we use the D4RL MuJoCo Gym dataset that contains three environments: *halfcheetah*, *hopper*, and *walker2d*. For each environment, there are six different behavior policy configurations: *random* (r), *medium* (m), *medium-replay* (mr), *medium-expert* (me), *expert* (e), and *full-replay* (fr).

4.1 CBOP CAN AUTOMATICALLY ADJUST RELIANCE ON THE LEARNED MODEL

To investigate RQ1, we use the notion of the *expected rollout horizon*, which we define as $\mathbb{E}[h] = \sum_{h=0}^H w_h \cdot h$. Here, w_h is the weight given to the mean of \hat{R}_h as defined in (8). A larger $\mathbb{E}[h]$ indicates that more weights are assigned to longer-horizon model-based rollouts.

Figure 1 already shows that $\mathbb{E}[h]$ decreases as the Q function becomes better over time. On the other hand, Figure 3 shows how the quality of the learned model affects $\mathbb{E}[h]$. Specifically, we trained the dynamics model on *halfcheetah-m* for different numbers of epochs (10, . . . , 100); then, we trained the policy with CBOP for 150 epochs.

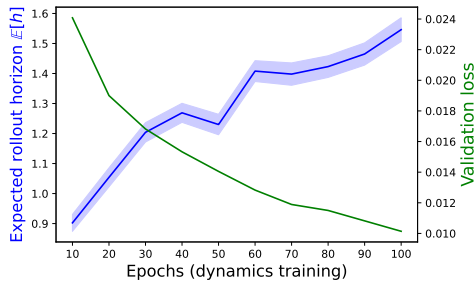


Figure 3: $\mathbb{E}[h]$ during CBOP training with the dynamics model trained for different numbers of epochs. CBOP can place larger weights to longer-horizon rollouts as the dynamics model becomes more accurate.

4.2 PERFORMANCE COMPARISON

To investigate RQ2, we select baselines covering both model-based and model-free approaches: (*model-free*) **CQL** (Kumar et al., 2020), **IQL** (Kostrikov et al., 2022), **TD3+BC** (Fujimoto & Gu, 2021), **EDAC** (An et al., 2021); (*model-based*) **MOPO** (Yu et al., 2020), **MOReL** (Kidambi et al., 2021), and **COMBO** (Yu et al., 2021). Details of experiments are provided in Appendix C.1.

Table 1 shows the experimental results. Comparing across all baselines, CBOP presents new state-of-the-art performance in **11 tasks out of 18** while performing similar in the remaining configurations. Notably, CBOP outperforms prior works in *medium*, *medium-replay*, and *full-replay* configurations with large margins. We maintain that these are the datasets of greater interest than, e.g., *random* or *expert* datasets because the learned policy needs to be much different than the behavior policy in order to perform well. Furthermore, the improvement compared to previous model-based arts is substantial: CBOP outperforms MOPO, MOReL, and COMBO by 116.4%, 23.2% and 23.7% (respectively) on average across four behavior policy configurations.

4.3 CBOP LEARNS CONSERVATIVE VALUES

To answer RQ3, we have selected 3 configurations (*m*, *me*, and *mr*) from the *hopper* environment and evaluated the value function at the states randomly sampled from the datasets, i.e., $\mathbb{E}_{\mathbf{s} \sim \mathcal{D}}[\hat{V}^\pi(\mathbf{s})]$ (nb. a similar analysis is given in CQL). Then, we compared these estimates with the Monte Carlo estimations from the true environment by rolling out the learned policy until termination.

Table 2: Difference between the values predicted by the learned Q functions and the true discounted returns from the environment.

Task name	CQL		CBOP	
	Mean	Max	Mean	Max
hopper-m	-61.84	-3.20	-55.83	-16.21
hopper-mr	-142.89	-28.73	-172.45	-39.45
hopper-me	-79.67	-5.16	-114.39	-11.24

Table 2 reports how large are the value predictions compared to the true returns. Notice that not only the mean predictions are negative but also the maximum values are, which affirms that CBOP indeed has learned conservative value functions. Despite the predictions by CBOP being smaller than those of CQL in *hopper-mr* and *me*, we can see that CBOP significantly outperforms CQL in these settings.

4.4 ABLATION STUDIES

LCB vs. MAP in the offline setting To answer RQ4, we compare CBOP with STEVE (Buckman et al., 2018) which corresponds to using the MAP estimation for target Q predictions. Figure 1 (left) shows the case where the value function learned by STEVE blows up. Further, we include the performance of STEVE in all configurations in Appendix D.2. To summarize the results, STEVE fails to learn useful policies for 11 out of 18 tasks. Especially, except for the *fr* datasets, using the MAP estimation has led to considerable drops in the performances in the *hopper* and *walker2d* environments, which reaffirms that it is critical to have the full posterior distribution over the target values such that we can make conservative target predictions.

Adaptive weighting For RQ5, consider an alternative way of combining $\hat{R}_h \forall h$ by explicitly assigning a fixed set of weights: uniform or geometric. We call the latter λ -weighting, in reference to the idea of TD(λ) (Sutton, 1988). We evaluated the performance of the fixed weighting scheme with various $\lambda \in (0, 1)$ values (Figure 4), and please see Appendix D.2 for the full results.

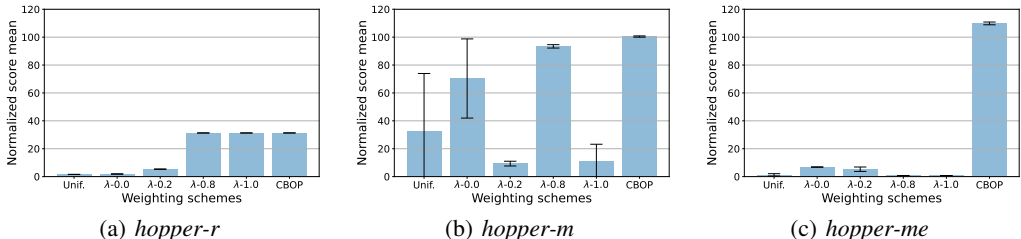


Figure 4: Performance comparison across different weighting schemes

In Figure 4(a), the performance improves as λ increases in *hopper-r*, suggesting that longer-horizon model rollouts helped. However, it is hard to pick a single λ that works across all environments. Thus, λ should be tuned as a hyperparameter; in contrast, CBOP can automatically adapt the horizon.

5 RELATED WORK

In the pure offline RL setting, it is known that the direct application of off-policy algorithms fails due to value overestimation and the resulting policy distribution shift (Kumar et al., 2019; 2020; Fujimoto & Gu, 2021; Yu et al., 2021). Hence, it is critical to strike the balance between *conservatism* and *generalization* such that we mitigate the extent of policy distribution shift while ensuring that the learned policy π_θ performs better than behavior policy π_β . Below, we discuss how existing model-free and model-based methods address these problems in practice.

Model-free offline RL *Policy constraint* methods directly constrain the deviation of the learned policy from the behavior policy. For example, BRAC (Wu et al., 2019) and BEAR (Kumar et al., 2019) regularize the policy by minimizing some divergence measure between these policies (e.g., MMD or KL divergence). Alternatively, BCQ (Fujimoto et al., 2019) learns a generative model of the behavior policy and uses it to sample perturbed actions during policy optimization.

On the other hand, *value regularization* methods such as CQL (Kumar et al., 2020) add regularization terms to the value loss in order to implicitly regulate the distribution shift (Kostrikov et al., 2021; Wang et al., 2020). Recently, some simple yet effective methods have been proposed. For example, TD3+BC (Fujimoto & Gu (2021)) adds a behavioral cloning regularization term to the policy objective of an off-policy algorithm (TD3 (Fujimoto et al., 2018)) and achieves SOTA performances across a variety of tasks. Also, by extending Clipped Double Q-learning (Fujimoto et al., 2018) to an ensemble of N Q functions, EDAC (An et al., 2021) achieves good benchmark performances.

Model-based offline RL Arguably, the learning paradigm of offline RL strongly advocates the use of a dynamics model, trained in a supervised way with a fixed offline dataset. Although a learned model can help generalize to unseen states or new tasks, model bias poses a significant challenge. Hence, it is critical to know when to trust the model and when not to. MOPO (Yu et al., 2020) and MOREL (Kidambi et al., 2021) address this issue by constructing and learning from a pessimistic MDP whose reward is penalized by the uncertainty of the state prediction. On the other hand, COMBO (Yu et al., 2021) extends CQL within the model-based regime by regularizing the value function on OOD samples generated via model rollouts.

Model-based value expansion Unlike Dyna-style methods that augment the dataset with model-generated rollouts (Sutton, 1990; Janner et al., 2019), MVE (Feinberg et al., 2018) uses them for better estimating TD targets during policy evaluation. While equally weighted h -step model returns were used in MVE, STEVE (Buckman et al., 2018) introduced an adaptive weighting scheme from the optimization perspective by approximately minimizing the variance of the MSBE loss, while ignoring the bias. Interestingly, the Bayesian posterior mean (i.e., the MAP estimator) we derive in (8) matches the weighting scheme proposed in STEVE. However as we show in Figure 1 and 9, using the MAP estimator as value prediction in the offline setting often results in largely overestimated Q values, which immensely hampers policy learning. See Section 3.1 for the related discussion.

6 CONCLUSION

In this paper, we present CBOP: conservative Bayesian model-based value expansion (MVE) for offline policy optimization. CBOP is a model-based offline RL algorithm that trades off model-free and model-based value estimates according to their respective epistemic uncertainty during policy evaluation while facilitating conservatism by taking a lower bound on the Bayesian posterior value estimate. Viewing each h -step MVE target as a conditionally independent noisy observation of the *true* target value under the learned MDP, we derive the Bayesian posterior distribution over the target value. For a practical implementation of CBOP, we use the ensemble of dynamics and that of Q function to sample MVE targets to estimate the Gaussian parameters, which in turn are used to compute the posterior distribution. Through empirical and analytical analysis, we find that the maximum

a posteriori (MAP) estimator of the posterior distribution could easily lead to value overestimation when the learned MDP is not accurate under the current policy. In contrast, CBOP enables using a lower confidence bound from the Bayesian posterior as a conservative estimation of the target value to successfully mitigate the issue while achieving state-of-the-art performance on several benchmark datasets.

REFERENCES

- Rishabh Agarwal, Max Schwarzer, Pablo Samuel Castro, Aaron Courville, and Marc G Bellemare. Deep reinforcement learning at the edge of the statistical precipice. *Advances in Neural Information Processing Systems*, 2021.
- Gaon An, Seungyong Moon, Jang-Hyun Kim, and Hyun Oh Song. Uncertainty-based offline reinforcement learning with diversified q-ensemble. In A. Beygelzimer, Y. Dauphin, P. Liang, and J. Wortman Vaughan (eds.), *Advances in Neural Information Processing Systems*, 2021. URL <https://openreview.net/forum?id=ZUvaSolQZh3>.
- Arthur Argenson and Gabriel Dulac-Arnold. Model-based offline planning. In *International Conference on Learning Representations*, 2021. URL <https://openreview.net/forum?id=OMNB1G5xz4>.
- James O Berger. *Statistical decision theory and Bayesian analysis; 2nd ed.* Springer series in statistics. Springer, New York, 1985. doi: 10.1007/978-1-4757-4286-2. URL <https://cds.cern.ch/record/1327974>.
- Robert N. Boute, Joren Gijsbrechts, Willem van Jaarsveld, and Nathalie Vanvuchelen. Deep reinforcement learning for inventory control: A roadmap. *European Journal of Operational Research*, 298(2):401–412, 2022. ISSN 0377-2217. doi: <https://doi.org/10.1016/j.ejor.2021.07.016>. URL <https://www.sciencedirect.com/science/article/pii/S0377221721006111>.
- Jacob Buckman, Danijar Hafner, George Tucker, Eugene Brevdo, and Honglak Lee. Sample-efficient reinforcement learning with stochastic ensemble value expansion. In *Proceedings of the 32nd International Conference on Neural Information Processing Systems, NIPS’18*, pp. 8234–8244, 2018.
- R. Christensen, W. Johnson, A. Branscum, and T.E. Hanson. *Bayesian Ideas and Data Analysis: An Introduction for Scientists and Statisticians*. Chapman & Hall/CRC Texts in Statistical Science. Taylor & Francis, 2011. ISBN 9781439803554. URL <https://books.google.ca/books?id=qPERhCbePNcC>.
- Kurtland Chua, Roberto Calandra, Rowan McAllister, and Sergey Levine. Deep reinforcement learning in a handful of trials using probabilistic dynamics models. In *Advances in Neural Information Processing Systems*, volume 31, 2018. URL <https://proceedings.neurips.cc/paper/2018/file/3de568f8597b94bda53149c7d7f5958c-Paper.pdf>.
- Richard Dearden, Nir Friedman, and Stuart Russell. Bayesian q-learning. *Aaai/iaai*, 1998:761–768, 1998.
- Vladimir Feinberg, Alvin Wan, Ion Stoica, Michael I. Jordan, Joseph E. Gonzalez, and Sergey Levine. Model-based value estimation for efficient model-free reinforcement learning, 2018.
- Justin Fu, Aviral Kumar, Ofir Nachum, George Tucker, and Sergey Levine. D4RL: datasets for deep data-driven reinforcement learning. *CoRR*, abs/2004.07219, 2020.
- Scott Fujimoto and Shixiang Gu. A minimalist approach to offline reinforcement learning. In A. Beygelzimer, Y. Dauphin, P. Liang, and J. Wortman Vaughan (eds.), *Advances in Neural Information Processing Systems*, 2021. URL <https://openreview.net/forum?id=Q32U7dzWXpc>.
- Scott Fujimoto, Herke van Hoof, and David Meger. Addressing function approximation error in actor-critic methods. In Jennifer G. Dy and Andreas Krause (eds.), *Proceedings of the 35th International Conference on Machine Learning, ICML 2018, Stockholm, Sweden, July 10-15, 2018*, volume 80 of *Proceedings of Machine Learning Research*, pp. 1582–1591. PMLR, 2018. URL <http://proceedings.mlr.press/v80/fujimoto18a.html>.
- Scott Fujimoto, David Meger, and Doina Precup. Off-policy deep reinforcement learning without exploration. In *Proceedings of the 36th International Conference on Machine Learning*, volume 97 of *Proceedings of Machine Learning Research*, pp. 2052–2062. PMLR, 09–15 Jun 2019. URL <https://proceedings.mlr.press/v97/fujimoto19a.html>.

- Tuomas Haarnoja, Aurick Zhou, Pieter Abbeel, and Sergey Levine. Soft actor-critic: Off-policy maximum entropy deep reinforcement learning with a stochastic actor. In *Proceedings of the 35th International Conference on Machine Learning*, volume 80 of *Proceedings of Machine Learning Research*, pp. 1861–1870. PMLR, 10–15 Jul 2018. URL <https://proceedings.mlr.press/v80/haarnoja18b.html>.
- Michael Janner, Justin Fu, Marvin Zhang, and Sergey Levine. When to trust your model: Model-based policy optimization. In *Advances in Neural Information Processing Systems*, 2019.
- Ying Jin, Zhuoran Yang, and Zhaoran Wang. Is pessimism provably efficient for offline rl? In Marina Meila and Tong Zhang (eds.), *Proceedings of the 38th International Conference on Machine Learning*, volume 139 of *Proceedings of Machine Learning Research*, pp. 5084–5096. PMLR, 18–24 Jul 2021. URL <https://proceedings.mlr.press/v139/jin21e.html>.
- Dmitry Kalashnikov, Alex Irpan, Peter Pastor, Julian Ibarz, Alexander Herzog, Eric Jang, Deirdre Quillen, Ethan Holly, Mrinal Kalakrishnan, Vincent Vanhoucke, and Sergey Levine. Scalable deep reinforcement learning for vision-based robotic manipulation. In *Proceedings of The 2nd Conference on Robot Learning*, volume 87 of *Proceedings of Machine Learning Research*, pp. 651–673. PMLR, 29–31 Oct 2018. URL <https://proceedings.mlr.press/v87/kalashnikov18a.html>.
- Rahul Kidambi, Aravind Rajeswaran, Praneeth Netrapalli, and Thorsten Joachims. Morel : Model-based offline reinforcement learning. In *Advances in Neural Information Processing Systems*, 2021.
- Ilya Kostrikov, Rob Fergus, Jonathan Tompson, and Ofir Nachum. Offline reinforcement learning with fisher divergence critic regularization. In Marina Meila and Tong Zhang (eds.), *Proceedings of the 38th International Conference on Machine Learning*, volume 139 of *Proceedings of Machine Learning Research*, pp. 5774–5783. PMLR, 18–24 Jul 2021. URL <https://proceedings.mlr.press/v139/kostrikov21a.html>.
- Ilya Kostrikov, Ashvin Nair, and Sergey Levine. Offline reinforcement learning with implicit q-learning. In *International Conference on Learning Representations*, 2022. URL <https://openreview.net/forum?id=68n2s9ZJWF8>.
- Aviral Kumar, Justin Fu, Matthew Soh, George Tucker, and Sergey Levine. Stabilizing off-policy q-learning via bootstrapping error reduction. In *Advances in Neural Information Processing Systems*, volume 32, 2019. URL <https://proceedings.neurips.cc/paper/2019/file/c2073ffa77b5357a498057413bb09d3a-Paper.pdf>.
- Aviral Kumar, Aurick Zhou, George Tucker, and Sergey Levine. Conservative q-learning for offline reinforcement learning. In *Advances in Neural Information Processing Systems*, 2020.
- Hoang Le, Cameron Voloshin, and Yisong Yue. Batch policy learning under constraints. In *International Conference on Machine Learning*, pp. 3703–3712. PMLR, 2019.
- Sergey Levine, Aviral Kumar, George Tucker, and Justin Fu. Offline reinforcement learning: Tutorial, review, and perspectives on open problems. *CoRR*, abs/2005.01643, 2020.
- Volodymyr Mnih, Koray Kavukcuoglu, David Silver, Andrei A. Rusu, Joel Veness, Marc G. Bellemare, Alex Graves, Martin Riedmiller, Andreas K. Fidjeland, Georg Ostrovski, Stig Petersen, Charles Beattie, Amir Sadik, Ioannis Antonoglou, Helen King, Dharmashan Kumaran, Daan Wierstra, Shane Legg, and Demis Hassabis. Human-level control through deep reinforcement learning. *Nature*, 518(7540):529–533, February 2015. ISSN 00280836. URL <http://dx.doi.org/10.1038/nature14236>.
- Paria Rashidinejad, Banghua Zhu, Cong Ma, Jiantao Jiao, and Stuart Russell. Bridging offline reinforcement learning and imitation learning: A tale of pessimism. In M. Ranzato, A. Beygelzimer, Y. Dauphin, P.S. Liang, and J. Wortman Vaughan (eds.), *Advances in Neural Information Processing Systems*, volume 34, pp. 11702–11716. Curran Associates, Inc., 2021. URL <https://proceedings.neurips.cc/paper/2021/file/60ce36723c17bbac504f2ef4c8a46995-Paper.pdf>.

- C. Robert. *The Bayesian Choice: From Decision-Theoretic Foundations to Computational Implementation*. Springer Texts in Statistics. Springer New York, 2007. ISBN 9780387715988. URL <https://books.google.ca/books?id=6oQ4s8Pq9pYC>.
- Richard S. Sutton. Learning to predict by the methods of temporal differences. *Machine Learning*, 3(1):9–44, August 1988. URL <http://www.cs.ualberta.ca/~sutton/papers/sutton-88.pdf>.
- Richard S. Sutton. Integrated architectures for learning, planning, and reacting based on approximating dynamic programming. In Bruce Porter and Raymond Mooney (eds.), *Machine Learning Proceedings 1990*, pp. 216–224. Morgan Kaufmann, San Francisco (CA), 1990.
- Richard S. Sutton and Andrew G. Barto. *Reinforcement Learning: An Introduction*. A Bradford Book, Cambridge, MA, USA, 2018. ISBN 0262039249.
- Ziyu Wang, Alexander Novikov, Konrad Zolna, Josh S Merel, Jost Tobias Springenberg, Scott E Reed, Bobak Shahriari, Noah Siegel, Caglar Gulcehre, Nicolas Heess, and Nando de Freitas. Critic regularized regression. In *Advances in Neural Information Processing Systems*, volume 33, pp. 7768–7778, 2020. URL <https://proceedings.neurips.cc/paper/2020/file/588cb956d6bbe67078f29f8de420a13d-Paper.pdf>.
- Larry Wasserman. *All of Statistics: A Concise Course in Statistical Inference*. Springer Publishing Company, Incorporated, 2010. ISBN 1441923225.
- Yifan Wu, George Tucker, and Ofir Nachum. Behavior regularized offline reinforcement learning. *CoRR*, abs/1911.11361, 2019. URL <http://arxiv.org/abs/1911.11361>.
- Fisher Yu, Wenqi Xian, Yingying Chen, Fangchen Liu, Mike Liao, Vashisht Madhavan, and Trevor Darrell. BDD100K: A diverse driving video database with scalable annotation tooling. *CoRR*, abs/1805.04687, 2018. URL <http://arxiv.org/abs/1805.04687>.
- Tianhe Yu, Garrett Thomas, Lantao Yu, Stefano Ermon, James Zou, Sergey Levine, Chelsea Finn, and Tengyu Ma. Mopo: Model-based offline policy optimization. In *Advances in Neural Information Processing Systems*, 2020.
- Tianhe Yu, Aviral Kumar, Rafael Rafailov, Aravind Rajeswaran, Sergey Levine, and Chelsea Finn. COMBO: conservative offline model-based policy optimization. *CoRR*, abs/2102.08363, 2021.

A ASSUMPTIONS

In this part, we discuss and analyze the core assumptions that we have made in the derivation and implementation of CBOP. First, recall that we view different h -step MVE returns \hat{R}_h for all $h = 0, \dots, H$ as *conditionally independent* observations of the true underlying parameter \hat{Q}^π . Second, we have modeled the likelihood of the observations with the Gaussian distribution with mean μ_h and standard deviation σ_h , which we estimate via sampling from the ensemble of dynamics and that of Q function. Third, we use the improper prior, which still provides us a proper posterior distribution that is also Gaussian. Below, we describe in more detail about each of these assumptions.

A.1 THE CONDITIONAL INDEPENDENCE ASSUMPTION

In order to meet the conditional independence assumption between \hat{R}_h , we need to estimate each \hat{R}_h with samples that are independently sampled. One way of achieving this is to generate samples per each h , resulting in an algorithm that requires $\mathcal{O}(NH^2)$ samples (and computation). However, we have found that there is no specific benefit in this computational intensive sampling procedure in terms of the final performance. Hence, our practical implementation only performs the forward sampling once, reducing the computational cost down to $\mathcal{O}(NH)$.

A.2 THE BAYESIAN POSTERIOR ESTIMATION

The improper prior assumption We have used the improper (or uninformative) prior in deriving CBOP in Section 3.1. Not to mention that the improper priors have been widely used in literature (Wasserman, 2010; Berger, 1985; Christensen et al., 2011), we further argue that it is quite natural (and sometimes necessary) not to assume any prior information if we are to apply our algorithm to general environments/tasks that have different dynamics. When some prior information is available, however, it is possible to incorporate it as long as we can use a conjugate prior that leads to a closed-form posterior update. It is critical to keep the posterior in closed-form since otherwise we have to resort to, e.g., posterior sampling, which will substantially (and unnecessarily) increase the computational footprint.

Empirical evidence supporting the Gaussian assumption over $\mathbb{P}(\hat{R}_h | \hat{Q}^\pi)$ First, note that the true return distribution should have a single peak in the locomotion environments we consider due to their deterministic nature, as long as the policy is deterministic. However, model-generated returns can have bimodality in their distributions since different models in the dynamics ensemble can lead to different trajectories, some of which can early terminate with low returns, while others continue to receive larger returns. Hence, it is interesting to examine whether it is reasonable to assume the Gaussian distribution over the h -step returns.

To answer this question, we have plotted the histograms of h -step returns for different h values in three tasks: *halfcheetah-mr*, *hopper-mr*, and *walker-mr*. Figure 5 (a)-(c) show that it is reasonable to assume \hat{R}_h are normally distributed. We have also observed that the empirical distribution of \hat{R}_h sampled from certain states can have bimodality (Figure 5d). Notice that the histograms are more spread out as h increases, which is due to compounded model errors. However, we note that the Gaussian distribution can still capture the support of the return distribution reasonably well.

The Gaussian likelihood assumption As discussed above and shown in Figure 5, the Gaussian assumption captures the actual return distributions reasonably well. Although it is possible to derive a closed-form posterior update in Student t distribution by making an additional assumption in the variance of \hat{R}_h likelihood (nb. we omit the actual derivation as it is not the contribution of this paper), we have observed that this does not lead to meaningful performance improvements compared to the much simpler Gaussian posterior that we derive in Section 3.1.

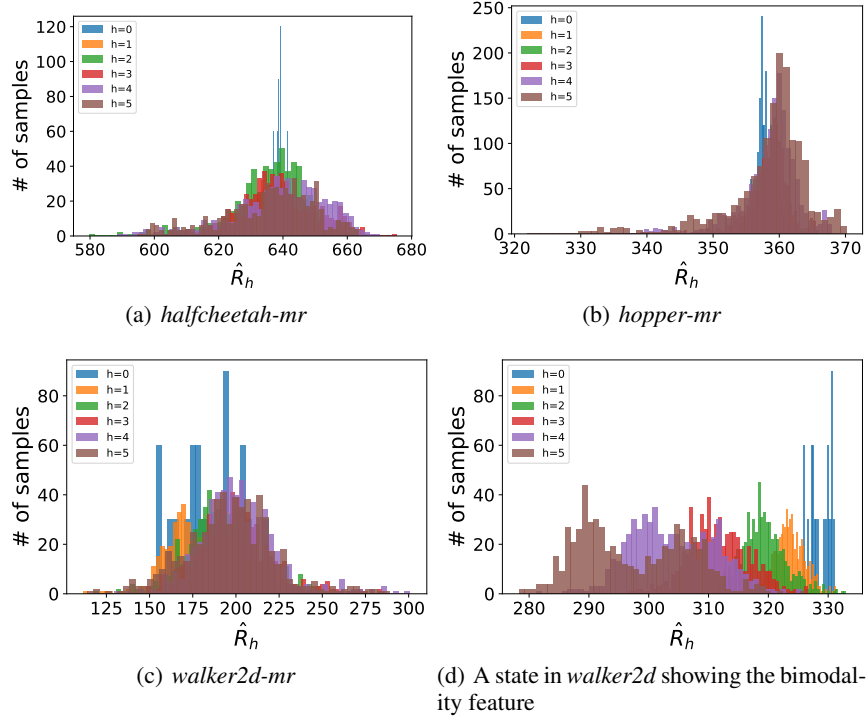
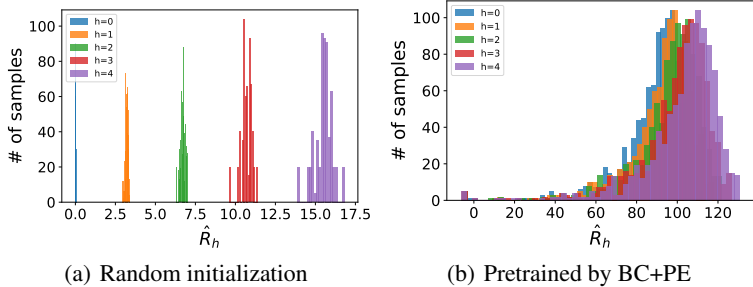


Figure 5: The histogram of $\hat{R}_h \forall h \in [0, 5]$ of a randomly selected state during training, evaluated across three locomotion environments with the *medium-replay-v2* configuration.

Algorithm 1 CBOP: Conservative Bayesian MVE for Offline Policy Optimization

- 1: **Input:** Data \mathcal{D} , discount factor γ , rollout horizon H , LCB coefficient ψ
 - 2: Initialize actor π_θ , Q ensemble Q_ϕ and target $Q_{\phi'}$, dynamics ensemble $\hat{f}_k = (\hat{T}_k, \hat{r}_k) \forall k$
 - 3: Pretrain \hat{f}_ξ on \mathcal{D} till convergence
 - 4: Pretrain π_θ and Q_ϕ on \mathcal{D} with BC and FQE respectively (Appendix B.3)
 - 5: **while** π_θ not converged **do**
 - 6: Sample a batch of transitions $B = \{\tau_i : \tau_i = (\mathbf{s}, \mathbf{a}, r, \mathbf{s}')\}_{i=1}^{|B|} \subset \mathcal{D}$
 - 7: **for** $\tau_i \in B$ **do** ▷ this step happens in parallel for all $\tau_i \in B$
 - 8: $\hat{\mathbf{s}}_0^k \leftarrow \mathbf{s}, \hat{\mathbf{s}}_1^k \leftarrow \mathbf{s}', \hat{\mathbf{a}}_0^k \leftarrow \mathbf{a}, \hat{r}_0^k \leftarrow r, \quad \forall k \in [1, K]$
 - 9: **for** $h = 0$ to H **do**
 - 10: **if** $h \geq 1$ **then**
 - 11: Sample an action $\hat{\mathbf{a}}_h^k \sim \pi_\theta(\hat{\mathbf{s}}_h^k) \forall k$
 - 12: Sample next state transition and reward $(\hat{\mathbf{s}}_{h+1}^k, \hat{r}_h^k) \leftarrow \hat{f}_k(\hat{\mathbf{s}}_h^k, \hat{\mathbf{a}}_h^k) \forall k$
 - 13: **end if**
 - 14: $\hat{R}_h^{k,m} \leftarrow \sum_{t=0}^h \gamma^t \hat{r}_t^k + \gamma^{h+1} \hat{Q}_{\phi'}^m(\hat{\mathbf{s}}_{h+1}^k, \hat{\mathbf{a}}_{h+1}^k) \quad \forall m$
 - 15: **end for**
 - 16: Compute μ_h and σ_h by (9) and (10), respectively
 - 17: Estimate μ, σ^2 of $\mathbb{P}(\hat{Q} | \hat{R}_0, \dots, \hat{R}_H) \sim \mathcal{N}(\mu, \sigma^2)$ by (8)
 - 18: Compute target Q value: $y_i(\mathbf{s}, \mathbf{a}, \mathbf{s}') \leftarrow \mu - \psi\sigma$
 - 19: **end for**
 - 20: Update π_θ and Q_ϕ following an off-policy actor-critic algorithm (e.g., SAC Haarnoja et al. (2018))
 - 21: Update the target network $Q_{\phi'}$
 - 22: **end while**
-

Figure 6: The histogram of $\hat{R}_h \forall h \in [0, 4]$ evaluated on *halfcheetah-medium-v2*

B ALGORITHM DETAILS

B.1 ALGORITHM SUMMARY

Algorithm 1 summarizes CBOP. In lines 20-21, we can use any off-policy actor-critic algorithm as the backbone of our approach, since the only part that changes is the computation of the target value $y(\mathbf{s}, \mathbf{a}, \mathbf{s}')$. In this work, we follow EDAC (An et al., 2021) — which builds on SAC (Haarnoja et al., 2018) — because it also employs Q ensembles. As discussed in Appendix B.3, a large discrepancy in the scale of the terminal $Q_{\phi'}$ predictions and that of the model-based rollout returns $\sum \gamma^t \hat{r}_t$ in the initial iterations greatly hampers policy learning. Hence, we pretrain the policy π_θ and Q_ϕ with with behavioral cloning (BC) and policy evaluation (PE) as elaborated in Appendix B.3.

B.2 DYNAMICS MODEL ARCHITECTURE

In this work, we approximate the true dynamics with a probabilistic ensemble model introduced by PETS (Chua et al., 2018). We follow the common configurations used in the literature, e.g., MBPO (Janner et al., 2019) and MOPO (Yu et al., 2020). Each model in the ensemble has 4 fully connected layers with 200 neurons. Specifically, we train the ensemble of 30 models, from which we select 20 models (often called ‘elite’) with smaller validation errors. For next state predictions, we train the ensemble model to predict the *delta* states, or $\Delta = \mathbf{s}' - \mathbf{s}$ for $(\mathbf{s}, \mathbf{s}') \in \mathcal{D}$. We normalize the inputs and outputs of the model for training and evaluation.

B.3 PRETRAINING

In some environments, we notice that training Q_ϕ and π_θ from scratch could be challenging, and Figure 6 illustrates the reason. Remember that we pretrain the dynamics ensemble with the offline data \mathcal{D} until convergence. Then, the reward predictions made by the model would have the proper scale. On the other hand, the $Q_{\phi'}$ ensemble is initialized with small random values. Hence, in the early iterations of policy learning, even though the Q_ϕ ensemble has not been trained yet, its predictions have a very small variance compared to the model-based rollout returns given by the learned dynamics ensemble (Figure 6(a)). This will then lead to all weights being concentrated on \hat{R}_0 , effectively MF; the MB rollouts would only slow down learning without contributing anything in this case. Besides, the variance of $Q_{\phi'}$ ensemble would be negligible, suggesting that taking the LCB would not introduce a sufficient level of conservatism into learning, which can hurt the performance.

Therefore in the experiments, we pretrain Q_ϕ and π_θ with the offline data. Specifically, we use behavior cloning (BC) for the policy network π_θ . In BC, we minimize the mean squared loss $\mathcal{L}_{\text{BC}} = \mathbb{E}_{(\mathbf{s}, \mathbf{a}) \sim \mathcal{D}} [(\mathbf{a} - \pi(\mathbf{s}))^2]$. For the value network Q_ϕ , we perform policy evaluation (PE) using Fitted Q-Evaluation (FQE) (Le et al., 2019). At each iteration k , FQE constructs a supervised learning dataset $\mathcal{D}^{(k)} = \{(\mathbf{s}_i, \mathbf{a}_i), y_i\}_{i=1}^n$ by estimating the target value y_i for each $(\mathbf{s}_i, \mathbf{a}_i) \sim \mathcal{D}$, with respect to the current Q approximation $Q_\phi^{(k-1)}$ and the associated transition tuple $(\mathbf{s}_i, \mathbf{a}_i, r_i, \mathbf{s}_{i+1}, \mathbf{a}_{i+1})$ using $y_i = r_i + \gamma Q_\phi^{(k-1)}(\mathbf{s}_{i+1}, \mathbf{a}_{i+1})$. We then train the Q function to minimize the MSE loss or

Table 3: The LCB coefficient ψ used in the D4RL MuJoCo Gym experiments.

Task Name	ψ		
	halfcheetah	hopper	walker2d
random	3.0	5.0	5.0
medium	0.5	3.0	3.0
medium-replay	0.5	2.0	3.0
medium-expert	3.0	3.0	3.0
expert	5.0	3.0	3.0
full-replay	0.5	3.0	0.5

$Q_\phi^{(k)} = \arg \min_\phi \frac{1}{n} \sum_{i=1}^n (Q_\phi^{(k-1)}(s_i, \mathbf{a}_i) - y_i)^2$. FQE iteratively repeats the above two steps to learn the Q ensemble model.

C EXPERIMENT DETAILS

C.1 EXPERIMENTAL SETTINGS

D4RL MuJoCo Gym We use the v2 version for each dataset as provided by the D4RL library (Fu et al., 2020). Following Algorithm 1, we pretrain Q_ϕ and π_θ with BC and FQE. The resulting policy and the Q ensemble are trained for 1,000 more epochs using CBOP. Table 1 reports the mean and standard deviation obtained from 5 random seeds.

Comparison of target Q values of MAP and CBOP (Figure 1(a)) In Figure 1(a), we compare the MAP estimation with the LCB in the *hopper-random* dataset. We have plotted the mean and \pm one standard error over the course of training. The MAP estimation simply uses the mean μ in (8) as the target $y(s, \mathbf{a}, s')$, whereas the LCB utilizes the variance of the posterior distribution to compute $y(s, \mathbf{a}, s') = \mu - \psi \cdot \sigma$. Note that we can also use other conservative estimate of the target using the posterior distribution; for example, we can use value-at-risk (VaR), conditional value-at-risk (CVaR) or other quantiles.

Expected rollout horizon of CBOP (Figure 1(b) and Figure 3) In Figure 1 and 3, we report the expected rollout horizon values. The expected rollout horizon can be computed per each sample in the batch during policy training, and we have reported the average value across all samples in a batch.

C.2 HYPERPARAMETERS

Table 3 summarizes the CBOP hyperparameters we use in the experiments presented in Section 4. The only hyperparameter that we have tuned is the LCB coefficient ψ , while we have used $H = 10$, $K = 20$, and $lr = 3 \times 10^{-4}$ for all experiments. We use $M = 20$ for *halfcheetah* and *walker2d*, and $M = 50$ for *hopper* environments. We use the final online evaluation performance in tuning the LCB parameter. We acknowledge that and we evaluated $\psi \in \{0.5, 2.0, 3.0, 5.0\}$ and selected

CBOP trades off the uncertainty of the learned dynamics model with that of the learned Q ensemble. In practice, we use the ensemble models to implicitly capture the respective epistemic uncertainty. Hence, it is critical that the models we use indeed exhibit well-calibrated uncertainty in their predictions. In this regard, we found that it is useful to incorporate the gradient diversification loss for the Q ensemble as introduced in An et al. (2021), which helps prevent the uncertainty in predictions from collapsing. Instead of tuning the hyperparameter η that controls the level of gradient diversification loss, we use a fixed number $\eta = 1$ across all experiments (except *walker2d-random* where we set $\eta = 50$).

Please note that the use of the ensemble diversification trick is orthogonal to our contributions in this work. Furthermore, we provide a reliable performance comparison between CBOP and EDAC to validate that CBOP outperforms EDAC. To this end, we use RLiab (Agarwal et al., 2021)

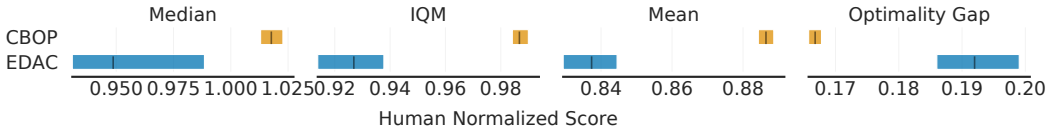


Figure 7: RLiable results across all 18 locomotion tasks. Shaded regions show 95% CIs. We refer readers to (Agarwal et al., 2021) for detailed explanation of the metrics considered.

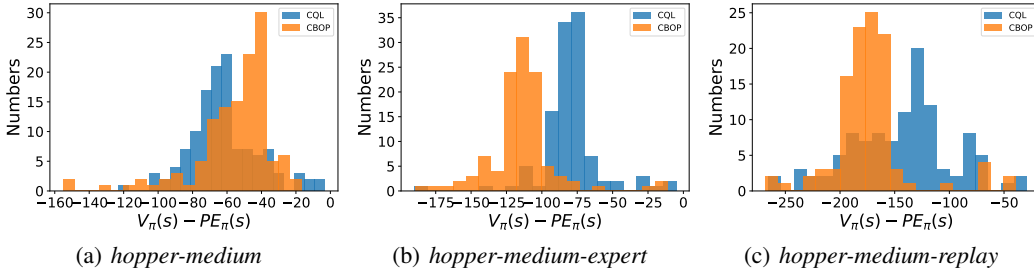


Figure 8: The distribution of difference between policy values predicted by algorithms and policy evaluation results, $s \sim \mathcal{D}, a = \pi(s)$.

which provides various metrics other than the simple average to more reliably determine the relative performances of compared methods. Specifically, we have reproduced EDAC and compared its performance against CBOP using the Median, IQM (interquartile mean), Mean, and Optimality Gap (Figure 7). In all metrics considered, CBOP exhibits substantially better performance without overlapping 95% confidence intervals (CI). In fact, another important performance metric, called the probability of improvement, of CBOP against EDAC is 88.27%, which strongly indicates the superiority of CBOP.

D ADDITIONAL EXPERIMENTS

D.1 CONSERVATISM ANALYSIS

We discuss the conservatism in CBOP in Section 4.3. Specifically, given the offline dataset \mathcal{D} , we have computed the following value difference:

$$\mathbb{E}_{s \sim \mathcal{D}} [\hat{V}^\pi(s) - \mathbb{E}[V^\pi(s)]] \quad (11)$$

where we compute the true value $\mathbb{E}[V^\pi]$ via the Monte Carlo estimation in the true environment. Table 2 shows the average and the maximum of this difference, while we provide the full histograms in Figure 8 comparing CBOP and CQL.

D.2 ABLATIONS

In this part, we provide additional ablations that complement the results presented in the main text.

The effectiveness of conservatism via LCB compared to MAP STEVE (Buckman et al., 2018) introduced an adaptive weighting scheme for MVE, which corresponds to the MAP estimation of the posterior we get in (8). In this part, we provide the complete ablations comparing CBOP and STEVE in all tasks.

In Figure 9(a), we see that STEVE performs comparably to CBOP in 4 of the 6 tasks, where small ψ have been used in CBOP (Table 3). However, for the *medium-expert* and *expert* tasks — where we have used $\psi = 3$ and 5, respectively — CBOP outperforms STEVE.

The differences in the performances are even more striking in the other two environments. Figure 9(b) and 9(c) show that CBOP significantly outperforms STEVE, suggesting that conservatism plays

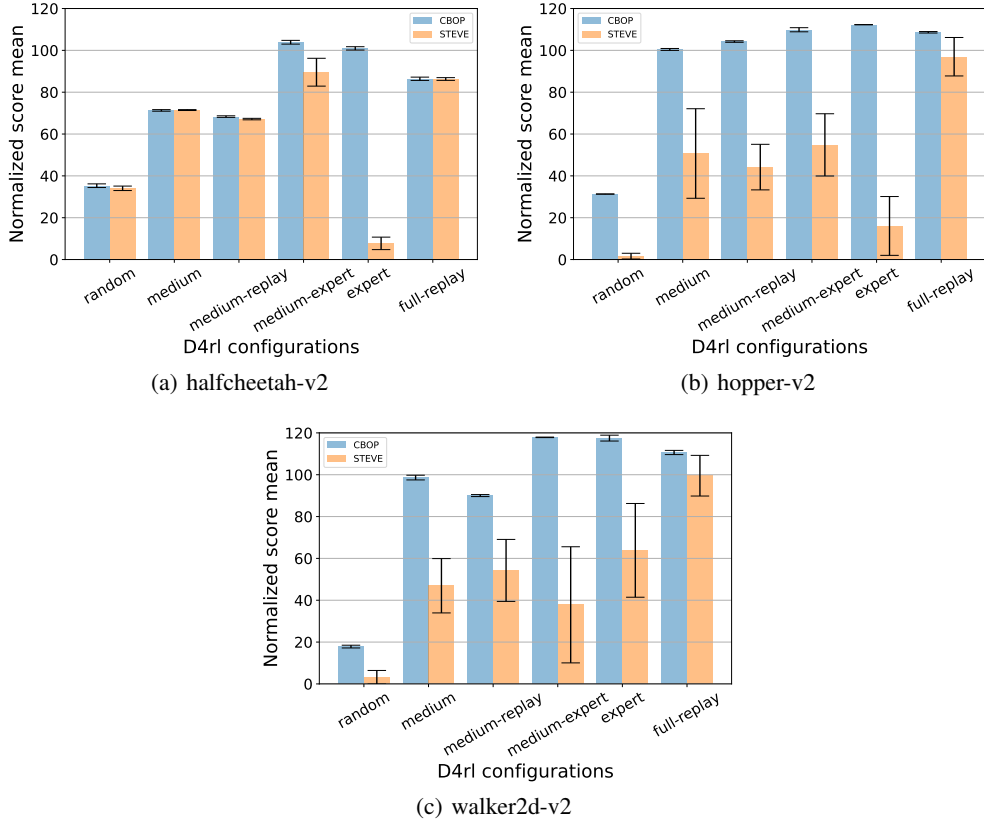


Figure 9: Comparison of the MAP estimation and the LCB estimation in the D4RL MuJoCo benchmark tasks. Experiments are run with 3 random seeds.

a crucial role. It is worth reasserting that the original adaptive weighting scheme derived in STEVE does not lend itself to a conservative value estimation as we can do with CBOP.

The effectiveness of the Bayesian weighting scheme In Section 4, we have presented a part of the ablations comparing the adaptive weighting scheme of CBOP with the fixed weighting scheme, i.e., uniform and λ weighting. The weights in the uniform weighting correspond to $w_h = \frac{1}{H+1}$, while those in the λ -weighting are $w_h = \frac{1-\lambda}{1-\lambda^{H+1}} \lambda^h$. In the latter, the larger the λ parameter, the more weight is allocated to longer-horizon model-based rollouts; $\lambda = 1$ corresponds to solely using the H -step MVE target, whereas $\lambda = 0$ bootstraps immediately at s' as in the model-free case.

In order to better isolate the impact of the different weighting schemes, we have used the conservative value estimation for these two fixed weighting schemes as well. More concretely, we have sampled $M \times K \hat{R}_h$ samples for $h = 0, \dots, H$ and computed the weighted sums ($\sum_{h=0}^H w_h \hat{R}_h$) to get MK samples of target values. With these samples, we have computed the empirical mean and the variance, from which we have taken the LCB $\mu - \psi \cdot \sigma$ as the target values.

Figure 10 - 12 show the results on the *halfcheetah*, *hopper*, and *walker2d* environments, respectively. We have found that the fixed weighting does not work in the *walker2d* tasks, regardless of the λ values. Also, CBOP has significantly outperformed the fixed weighting schemes in narrow datasets (i.e., *medium-expert*) across all environments.

In some tasks — such as *medium* and *medium-replay* tasks in *hopper* and *halfcheetah* environments, there are some λ values that can show similar performances as CBOP. However, large fluctuations across different λ values as exhibited in *halfcheetah-medium* and *hopper-medium* suggest that finding λ that works robustly across all tasks may be impossible. On the contrary, the adaptive Bayesian weighting scheme of CBOP can work reliably across all tasks considered.

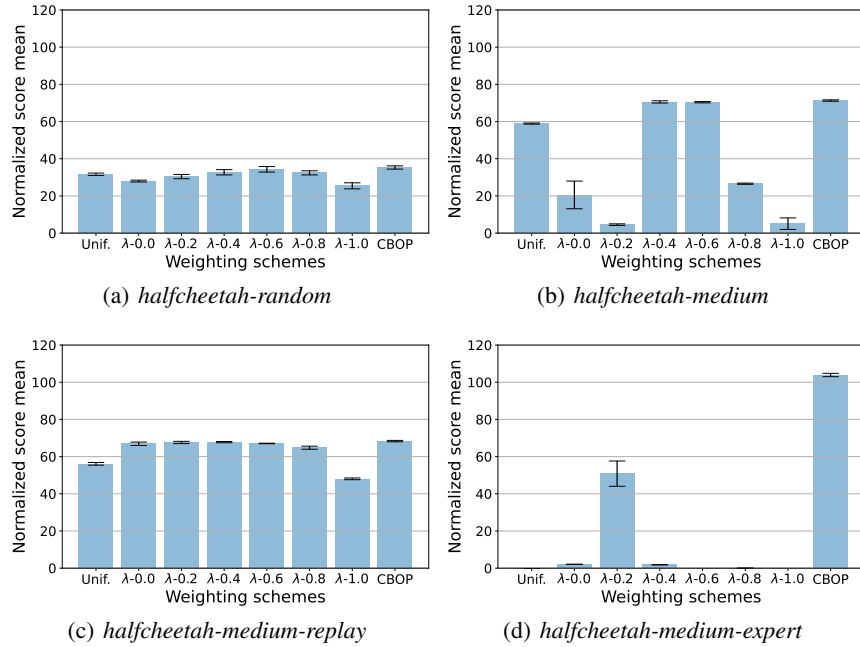


Figure 10: Comparing the fixed weighting schemes and CBOP on the *halfcheetah* environment. Experiments are run with 3 seeds.

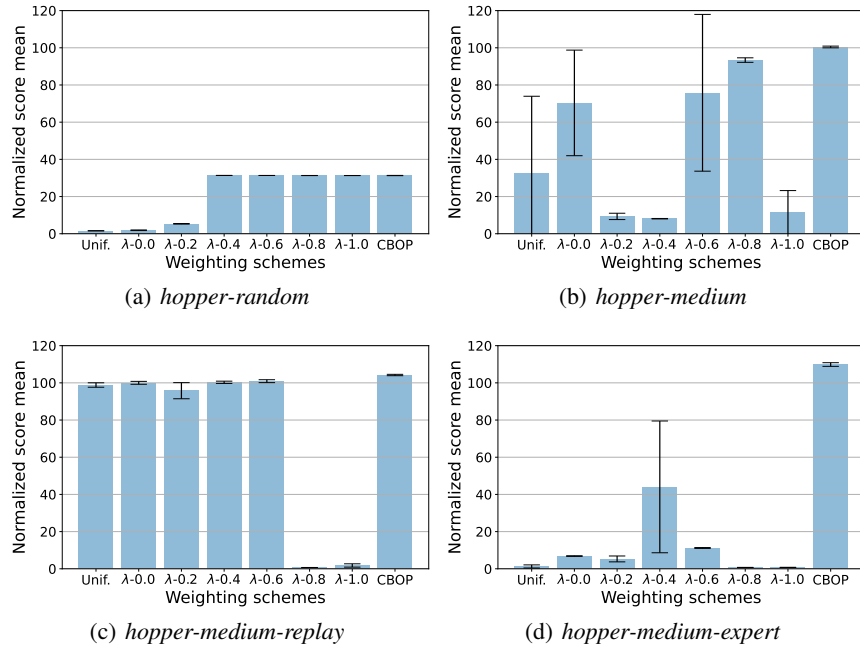


Figure 11: Comparing the fixed weighting schemes and CBOP on the *hopper* environment. Experiments are run with 3 seeds.

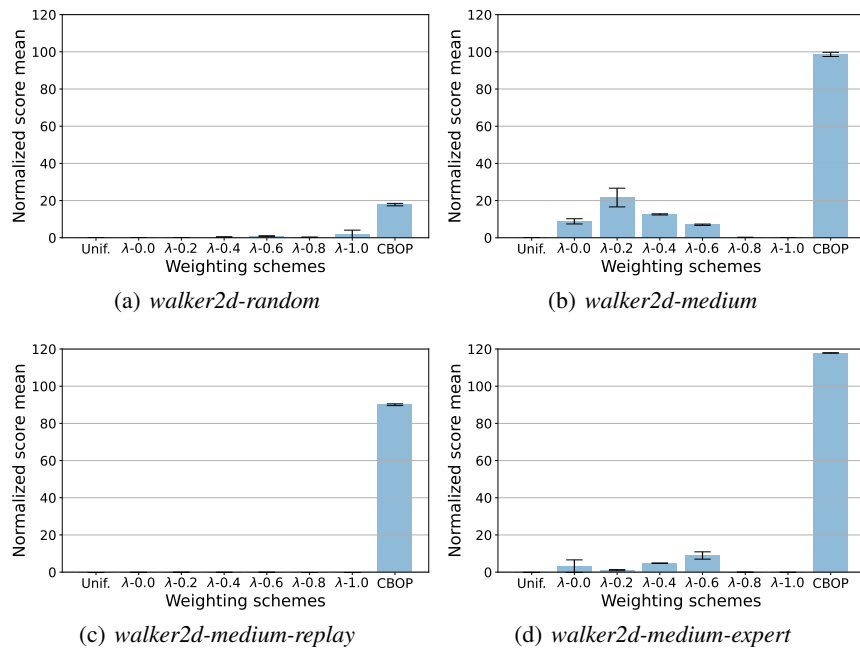


Figure 12: Comparing the fixed weighting schemes and CBOP on the *walker2d* environment. Experiments are run with 3 seeds.